

Optimization of Ingot Quality Using Evolutionary Algorithms

Petr Kotas*, MAGMA Giessereitechnologie GmbH, Kackerstrasse 11, D-520 72, Aachen, Germany, **Tomáš Huczala** and **Bohuslav Chmiel**, TRINECKÉ ŽELEZÁRNY, a.s., Průmyslová 1000, 739 70 Třinec, Czech Republic, **Jesper Henri Hattel**, Technical University of Denmark, Department of Mechanical Engineering, 2800 Kgs. Lyngby, Denmark
P.Kotas@magma-soft.cz

This paper presents findings and results of a fully coupled 3-D numerical simulation of the manufacturing process of a three ton large steel ingot. Simulation of the teeming process as well as several thermal criterion functions together with solidification calculations are utilized for predicting the occurrence and distribution of various casting discontinuities and defects such as shrinkage and centerline porosity inside the considered ingot. The original ingot layout and its process parameters are then subjected to fully automated computer optimization. This is accomplished by coupling the casting simulation software package MAGMASOFT® with an optimization engine based on genetic algorithms. The simulation package is used as a virtual experimentation field in which the optimizer varies process parameters or design features and in this way tries to find the optimal route to satisfy the given objective(s). Several parameters can be modified and evaluated independently of each other. The optimizer tries to find the best compromise to the given (mostly conflicting) objectives using simulations based on validated physics. This not only further reduces the need for physical trial runs to find the optimal process window, but allows for the detailed evaluation of many process parameters and their individual impact on providing a robust process. An optimization case is considered in which unknown optimal process parameters and boundary conditions, i.e. initial pouring temperature, pouring conditions, interface heat transfer coefficients, together with shapes and sizes of the hot top, its insulation and the mould taper, are sought using multi-objective genetic algorithms. All this is done in order to establish a more directional and progressive solidification and better thermal conditions inside the ingot to minimize the aforementioned defects.

Keywords: numerical optimization, steel ingots, heat transfer coefficients

1. Introduction

In recent years, the usage of simulation software has continuously increased and now integrates parallel processing computers. It is feasible to calculate numerous versions and layouts in almost unlimited configurations. The advantage of having such short calculation times can only be utilized provided that a computer can automatically analyze calculated variants with respect to predefined objectives (e.g. maximum feeding, low porosity, low air entrapment, etc.) and subsequently create new variants and analyze them in the same manner to achieve the optimal solution. Despite relatively high computational expenses, the autonomous integration of casting process simulations with numerical optimizations methodologies has recently been initiated, and it has been taken up not only by researchers but in practice in manufacturing [1- 7]. By integrating such software for casting process simulation with an optimization algorithm, a computer based optimization tool is established, which is able to determine optimal values of user defined design variables, thereby optimizing a given casting process with respect to predefined objectives. Several parameters, boundary and initial conditions, geometrical features, etc. can be changed at the same time and be evaluated independently from each other.

Autonomous optimization tools combine the classical approach of foundry engineers to find the ‘best compromise’ with validated physics. This not only further reduces the need for trial runs to find the optimal process window but also allows an in-depth evaluation of many parameters and their individual impact on providing a robust process. Subsequently, such system can readily provide optimal solutions for any kind of casting processes.

In the present paper, the original ingot casting layout is shape optimized where unknown optimal shapes of the ingot body (bottom and top diameters), its hot top and various process parameters such as pouring temperature and flow rate profile are sought by means of autonomous optimization to establish a better solidification pattern of the ingot, which would eliminate the likelihood of feeding related issues like shrinkage porosity and temperature gradient related defects such as centerline porosity. Despite having multiple targets to achieve, this issue is addressed by defining the problem as a single-objective optimization problem via combining one objective (minimization of shrinkage porosity) with multiple constraints, i.e. the presence of centerline porosity and establishment of directional and progressive solidification pattern inside the given ingot. The multi-objective genetic algorithm (MOGA) has been applied inside the optimization module MAGMAfrontier [8] to handle this single-objective problem.

2. Methods

2.1 Design of the ingots layout

The present study considers a cluster of four cylindrical steel ingots (total weight 12 tons, maximum dimensions $H=2100\text{mm}$, $D_{\text{bottom}}=473\text{mm}$, $D_{\text{top}}=457\text{mm}$, $H/D \text{ ratio}=4,52$, $\text{conicity}=-0,38$), $D_{\text{hot top}} = 410\text{mm}$, $H_{\text{hot top}} = 250\text{mm}$, shown in **Fig. 1**, made of X10CrMoVNb9-1 (DIN 1.4903) steel alloy. For simplicity, the original ingot will be called A-shape ingot, because its shape actually resembles letter A (due to its negative conicity). The reason for having the ingot with a negative conicity is that stripping of the given ingot type is much easier than for the ingot with positive conicity.

The ingot head (hot top) is completely surrounded by the exothermic brick-padding. The original ingot layout is bottom-filled assuming an initial pouring temperature of 1560°C (2840 deg. F) and a constant flow rate of 1t/min during the entire filling stage. The dies and the pouring tower are made of GJL-400 cast iron with an initial temperature of 40°C (104 deg. F). After teeming, the free surface is covered by exothermic powder to induce a favorable thermal gradient. All this information has been subsequently applied in the numerical simulation.

Afterwards the ingot has been sectioned along its entire height to carry out various measurements of macro segregation profiles of various elements, see **Fig. 2**. Besides the aforementioned measurements which are not presented in this study, the major use of the sectioned ingot has been to analyze and measure the magnitude of the internal defects such as centerline porosity and shrinkage porosity, see **Fig. 3**. This information is then used to calibrate the numerical simulation, as will be shown later in the text. **Fig. 3** shows that the porosity can be found almost along the entire height. The bottom part and the hot top are not considered, they have been cut off as implied in **Fig. 2**.

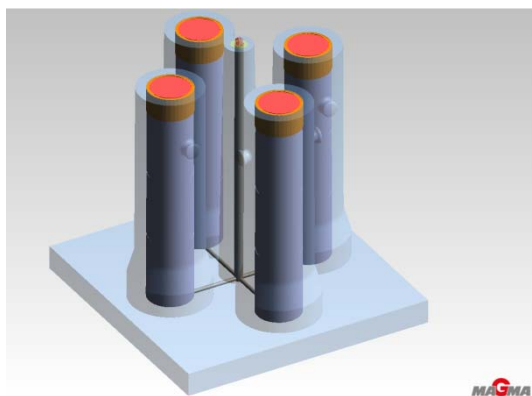


Fig. 1 The considered cluster of four ingots (Courtesy of Trinecke zelezarny, a.s.).

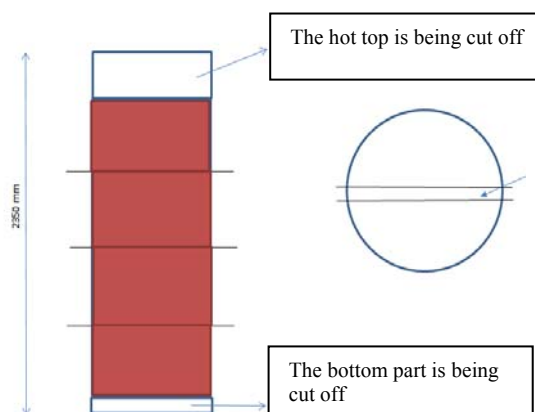


Fig. 2 Sketch of how the ingot has been sectioned for further analysis and comparison with the simulation results.



Fig. 3 Results from casting trial showing presence of porous areas and microstructure of the ingot (Courtesy of Trinecke zelezarny, a.s.). The bottom of the ingot is on the left hand side of the image.

The primary reason for performing the numerical optimization is to minimize the shrinkage porosity. It is clear that it may be impossible to completely avoid it, but its reduction in its diameter would be a success for the manufacturing foundry. The reason is that the center of this ingot is drilled away along its height and subsequently processed with rolling or forging operations. Nowadays, due to the magnitude of the defect, the foundry has to use a $\varnothing=90\text{mm}$ drilling tool to completely drill out the porosity. The foundry has a maximum $\varnothing=50\text{mm}$ drilling tool and therefore has to outsource this job. It is costly and time-consuming. The aim is to reduce the diameter of the shrinkage porosity below 50mm so that the foundry can perform the drilling operation in-house, saving time and money.

2.2 Model and Simulation Set-Up

The simulation of the ingot casting process at hand is carried out in the FVM-based software package MAGMA⁵ and in essence consists of mould filling and solidification. During mould filling the flow field is found from solving the momentum equations and the continuity equation under the assumption of a Newtonian fluid and incompressibility, which in turn is combined with the energy equation including convective terms in order to obtain the temperatures during teeming. This is followed by the solidification analysis in which the energy equation is solved in combination with the release of latent heat. It should be emphasized that during solidification the convective terms account for the natural convection taking place and as such they might have a considerable effect on the thermal fields for solidification of especially large cast parts like the one considered in the present work. During the optimization runs the natural convection is neglected such that only the reduced version of the heat conduction equation is solved here. This results in a considerable simplification of the problem and hence reduction in calculation time of the calculated scenarios during optimization. This procedure however still results in the right tendencies such that optimal solutions can be found.

When it comes to heat flow and its effect on the solidification behavior of slim and tall ingots, this work is based on findings of Hahn and Hepp [9]. Their paper clearly shows that the heat transfer between the solidifying ingot shell and the inner mould varies depending on the actual position between the bottom and the top of the ingot. They demonstrated that in order to properly describe the solidification of slim and tall ingots, it is necessary to vary the heat transfer coefficients over the height of the ingot. The given concept is depicted in **Fig. 4**. One should bear in mind that the step-like curve for the height-dependent heat transfer coefficients is just a simplified curve used for explaining the concept of the height-dependency of the heat transfer coefficients. In reality, the heat transfer coefficients are not constant even inside the given segments but continuously vary with both, the height and the temperature. In the simulations considered in this work, the simplified step-like curve for the height-dependent heat transfer coefficients was applied.

Hahn and Hepp [9] used an optimization engine based on genetic algorithms coupled with a casting process simulation package to seek the optimal height-dependent heat transfer coefficients which then minimize the deviations between the measured (experimentally acquired) and simulated cooling curves from the given ingot; see **Fig. 5** taken from their paper [9]. By carrying out the inverse optimization, a significant variation of the heat transfer coefficient over the height of the given ingot was determined. They also reported that these variations in the heat transfer coefficients over the ingot height led to more realistic predictions of thermal fields with subsequent defects such as centerline shrinkage in the ingot body as compared to the case study where a constant heat transfer coefficients over the height was applied see **Fig. 1** and **Fig. 4** in their paper [9].

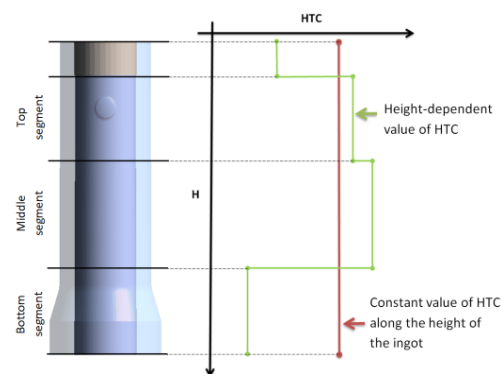


Fig. 4 The concept of height-dependent heat transfer coefficients. The red line represents a constant heat transfer coefficient that is widely applied for the simulation of ingots. The green step-like curve shows a distribution of heat transfer coefficients along the ingot height.

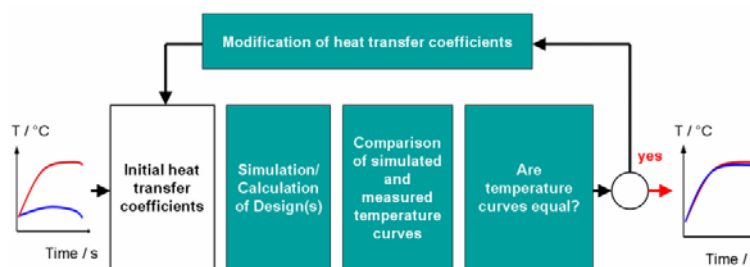


Fig. 5 Inverse analysis of heat transfer coefficients - By variation of the heat transfer coefficients between the ingot and the mould, the mould temperatures are varied. With a program for automatic optimization of casting processes, the deviation between the curvatures of simulated and measured temperatures on the outer surface of the mould can be minimized. Usually, several hundreds of simulations with different heat transfer are carried out until the simulated cooling curves fit to the measured ones. The heat transfer coefficients that correspond to the best fit can then be used for a realistic evaluation of the ingot solidification [9].

Thanks to the similarity in the ingot shape and its volume with the ingot used by Hahn and Hepp [9], findings concerning the height-dependent heat transfer coefficients from [9] are applied in this case study. The 3D CAD model of the considered ingot has been split into three sections along the height, see **Fig. 4** and each section has been allocated a unique value of a heat transfer coefficient, see **Table I**. The values of the height-dependent heat transfer coefficients have been adopted from the paper by Hahn and Hepp [9].

Due to the geometrical symmetry of the test ingot cluster, only one half of the geometry was considered during the simulations. The program then assumes symmetry at the surface where the virtual division plane cuts through the geometry. This means that there is no mass and heat transfer across this surface. An outline of the simulation analyses performed at various stages of this project is given in **Table II**.

Table I. – Height dependent Heat Transfer Coefficients adopted from the work by Hahn and Hepp [9] used for simulation.

Heat transfer coefficient [W/m ² K]	Ingot_bottom - Mould	300
	Ingot_middle – Mould	600
	Ingot_top - Mould	400

Table II. – Indication of the differences in complexity of the simulation analyses for the original and final layouts as compared to the optimization procedure.

	Filling	Solidification	
		Thermal analysis	Convection, macrosegregation
Original ingot layout	YES	YES	YES
Optimization procedure	YES	YES	NO
Optimized ingot layout	YES	YES	YES

3. Optimization methodology

When autonomous optimization is utilized, the user defines not only the degrees of freedom for the process parameters, geometrical features etc., but also a number of objective functions which may be conflicting and are to be either minimized, maximized, or a combination of these.

The actual optimization cycle is initiated by establishing a first generation, i.e. virtual set of experiments, containing a user-defined amount of individuals, referred to as initial population or Design Of computational Experiments (DOE). Each individual represents one configuration for the considered set of design variables. For each of these designs analyses of teeming and solidification are performed and the values for the requested output variables are calculated. The output data is used to evaluate and compare the different designs. After the first generation has been calculated, the optimization algorithm evaluates the designs with respect to the objective functions and constraint(s) and subsequently generates a new set of solutions using mathematical mechanisms that follow the concept of natural genetics, i.e. selection, reproduction, cross-over and mutation. Each time, the algorithm decides if a layout is kept, eliminated or modified – or if it is combined with an already calculated or new design. This iterative evolution strategy is consequently referred to as a Genetic Algorithm [10].

An effective type of the aforementioned genetic algorithm is MOGA, the multi-objective genetic algorithm. This algorithm has two features, being of particular importance in the context of casting simulation: It supports tracking of several independent objectives and can handle any type of process and design variables, even those variables occurring in casting simulation. MOGA is the applied algorithm in this study.

3.1 Problem Statement – Optimization of process conditions

The optimization problem here is defined as the goal of finding the most suitable set of process parameters and geometrical features of the given ingot layout. These are, (i) having the ingot sound (i.e. with minimum shrinkage porosity), (ii) at the same time establishing more directional and progressive solidification pattern in the ingot (iii) reducing the centerline micro porosity. In this study, only the minimization of the macroscopic shrinkage porosity is treated as an objective (single objective optimization problem) for easier visualization whereas the micro porosity and the directional solidification pattern were treated as constraints. The reason for defining the optimization problem as a single objective problem, although there is more than one goal to address, was that the considered objectives are not in conflict with each other, i.e. if there is a gain in one objective, there must be a sacrifice in the other one(s). In order to perform quality multi-objective optimization, the objectives at hand must be conflicting.

Since a shrinkage-free casting is desired, the porosity requirement in the ingot body is $Porosity_{critical} = 0\%$. Using the output results provided by the simulation software, the shrinkage porosity measure, $Porosity$ is taken as the maximum value contained in each of the control volumes of the ingot body. In total, 11 independent design variables are used in the optimization procedure: flow rate profile during teeming (altogether 7 design variables), see **Fig. 6**, dimensions of the hot top – its height, bottom and top diameters, pouring temperature, bottom and top

diameters of the ingot (altogether 6 design variables). Upper and lower limits for each process and design parameter varied are defined, see **Table III**.

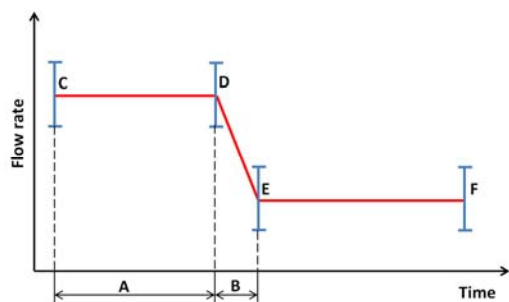


Fig. 6 Sketch of a typical flow rate profile during teeming of an ingot. Characters A - F indicate groups of design variables which are subjected to numerical optimization.

Table III Variations and degrees of freedom for the autonomous optimization

Design variable	Lower and upper boundaries
Filling temperature	1540-1590° C
Flow rate	0,6-1,2 t/min
D_ingot_bottom	457mm ÷ 493mm
D_ingot_top	457mm ÷ 493mm
D_hot top_bottom	410mm ÷ 493mm
D_hot top_top	410mm ÷ 493mm
Height_hot top	200mm ÷ 270mm

Dimensional constraints were imposed to the selected design variables to maintain realistic shapes of the hot top. Other constraints express goals of (a) having the centerline shrinkage less critical in the optimized ingot than in the original and (b) having favorable directional solidification pattern over the ingot height. Note that the only direct comparison of the optimized and real-casting results for the steel ingot (for centerline shrinkage) is possible for the vertical section cut of the ingot body, see **Fig. 2** and **3**, thus the focus is on that area.

The initial population of designs for the given optimization case for the multi-objective genetic algorithm containing 100 unique designs are provided by the quasi-random Sobol DOE sequence generating technique. Altogether 8 generations are run, giving a total number of 800 calculated solutions (designs).

4. Results and discussion

In the following sections, the results obtained from the simulations and casting trials are presented and discussed. First, the numerical and experimental results from the original ingot casting assembly are analyzed to establish a base case. Then, the results from the single objective optimization problem (process conditions optimization) are presented.

4.1 Casting and Simulation Results — Original Process Parameters

The analysis of the teeming process provides proper temperature fields inside the ingot for the subsequent solidification analysis. For ingots, due to very long teeming times it is absolutely necessary to consider teeming during simulations. Neglecting teeming would lead to false results inconsistent with the reality. Nevertheless, due to the extent of the paper, the results of the teeming process are neither shown nor discussed in this paper. The thermal analysis during solidification in essence evaluates the efficiency of the hot top, the cooling ability of the mould and the effect of the temperature fields on internal defects occurrence.

The ingot in **Fig. 7** is a good example of how geometry can lead to an improper, i.e. non-directional, solidification pattern, induce low pressure and thermal gradients and hence promote solidification related defects, i.e. centerline porosity. Due to the inability of the hot top to feed the entire height of the casting and due to the air gap which blocks the heat removal at the interface ingot-mould, progressive solidification could not have been established and thus solidification propagated only from the ingot walls inwards eventually choking off small liquid pools almost over the entire height of the ingot. These isolated pools did not have a chance to compensate for the volumetric shrinkage during the temperature drop which resulted in centerline shrinkage in the problematic area, see **Fig. 8(a-d)**. It must be noted that the prediction of choking of the residual liquid is possible only due to the use of height-dependent heat transfer coefficients. With the consideration of the constant heat transfer coefficient, no isolation of residual liquid has been observed.

Fig. 8(a) describes the situation from **Fig. 7** with the use of a single criterion Solidification time. It shows how long it took various areas of the ingot to cool from the pouring temperature to the solidus temperature. It is now evident that the ingot geometry, i.e. the A shape of the ingot, together with other process parameters will lead to choking off areas with residual liquid which will then give rise to shrinkage defects such as centerline shrinkage, see **Fig. 8(d)**. Part of the optimization study will be to look for the optimal ingot shape which would force the bottom part to solidify earlier than the top regions and hence impose directional and progressive solidification pattern.

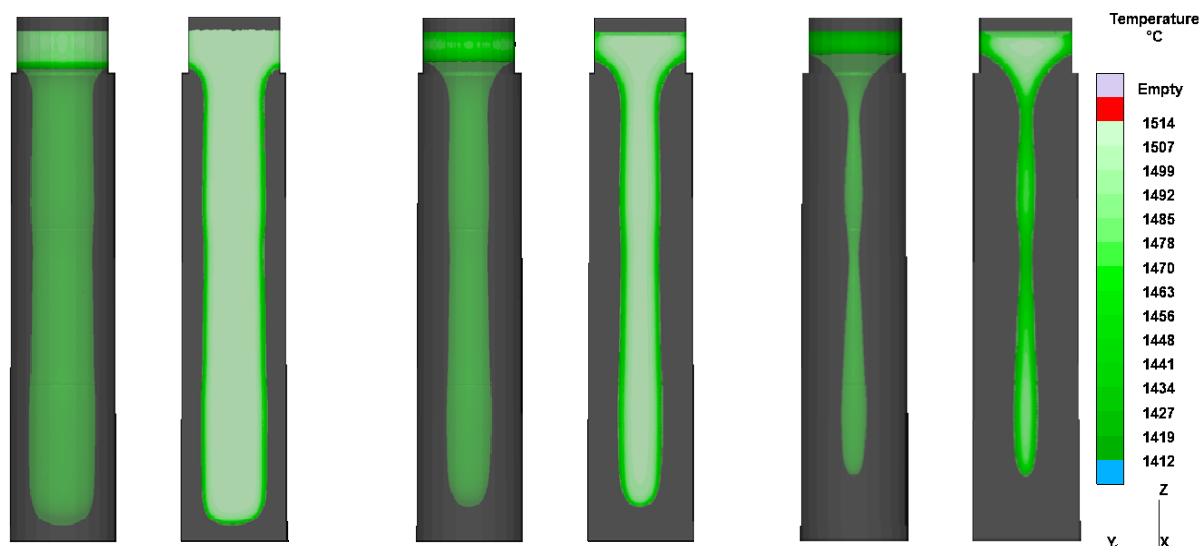


Fig. 7 Solidification processing showing strictly parallel movement of the isotherms and hindered solidification at the bottom of the ingot leading to choking of pools with residual liquid at various areas of the ingot. This is a natural consequence of both, the height-dependent heat transfer coefficients and the given geometry of the ingot having the bottom region larger than the top region, the so-called A-shaped ingot.

Fig. 8(b) shows the numerically predicted presence and magnitude of centerline porosity in the ingot body using the Niyama criterion. Since the critical value of this criterion is chemistry dependent, it was first necessary to determine this value for the considered steel alloy. This was done by measuring the actual size and the location of the defect inside the real ingot, **Fig. 3**. Having that information, the numerical scale for the Niyama criterion was adjusted inside the simulation software to reach the similar size and location of the defect as in the real ingot. A good correlation was found for the Niyama threshold value of approximately 1 for this particular steel alloy, however, it should be emphasized that the geometrical extension of the numerically-obtained centerline porosity is to some extent approximate due to its dependency on the chemistry. Shrinkage porosity predicted by the Niyama criterion usually forms in the mushy region at high solid fractions. At lower solid fractions, the pressure drop which governs this type of porosity is negligibly small. Therefore, in a casting simulation, the Niyama criterion is always evaluated at a temperature near the end of the solidification interval. With the help of the Niyama criterion, it is feasible to predict the presence of centerline shrinkage porosity, i.e. micro- and macro-shrinkage in alloys with short freezing range such as steels, caused by shallow temperature gradients. A low thermal gradient implies that even if liquid metal is available at a neighboring region, there is insufficient thermal ‘pressure’ for the flow to actually take place

Fig. 8(c) depicts more or less the same as the previous image, **Fig. 8(b)**. The predicted microporosity is based on the “modified” Niyama criterion developed by Carlson and Beckermann [11]. The original Niyama criterion accounts for thermal conditions, i.e. cooling rate and thermal gradient, but it does not account for the effect of the thermal conditions on the SDAS, which can significantly affect the resulting pore volume. If proper modifications are done, the “modified” Niyama criterion can easily account not only for the local thermal conditions considered by the original Niyama criterion, but also for the properties and solidification characteristics of the alloy and the critical pressure drop across the mushy zone for forming centerline shrinkage. The difference from the original Niyama criterion in the dependence on thermal conditions is due solely to the SDAS and the effect that this arm spacing has on the permeability in the mushy zone [11]. The Niyama criterion does not provide the actual amount of shrinkage porosity that forms, other than in a qualitative fashion (i.e., the lower the Niyama value, the more shrinkage porosity forms), while the Microporosity criterion based on the modified Niyama shows the predictions in a quantitative fashion. It gives the user an immediate answer as to how much material in % is missing in the given region or control volume of the mesh.

Fig. 8(d) indicates a result of the unfavorable solidification pattern, the macroscopic shrinkage porosity. The magnitude of the defect in the real ingot sentences the foundry to use expensive drilling tools ($\varnothing = 90\text{mm}$) as well as to outsource the job, to completely remove this defect. The main aim of the foundry for the optimization is to try to reduce the centerline macroscopic shrinkage below $\varnothing = 50\text{mm}$ so that the drilling operations can be done in-house and not outsourced as with the $\varnothing = 90\text{mm}$ defect. Besides the visual information about the size of the defect, a quantitative information about its volume [mm^3] as shown in **Fig. 8(d)** is available to the user. The volumes of the porous regions can then be compared with the optimized solution.

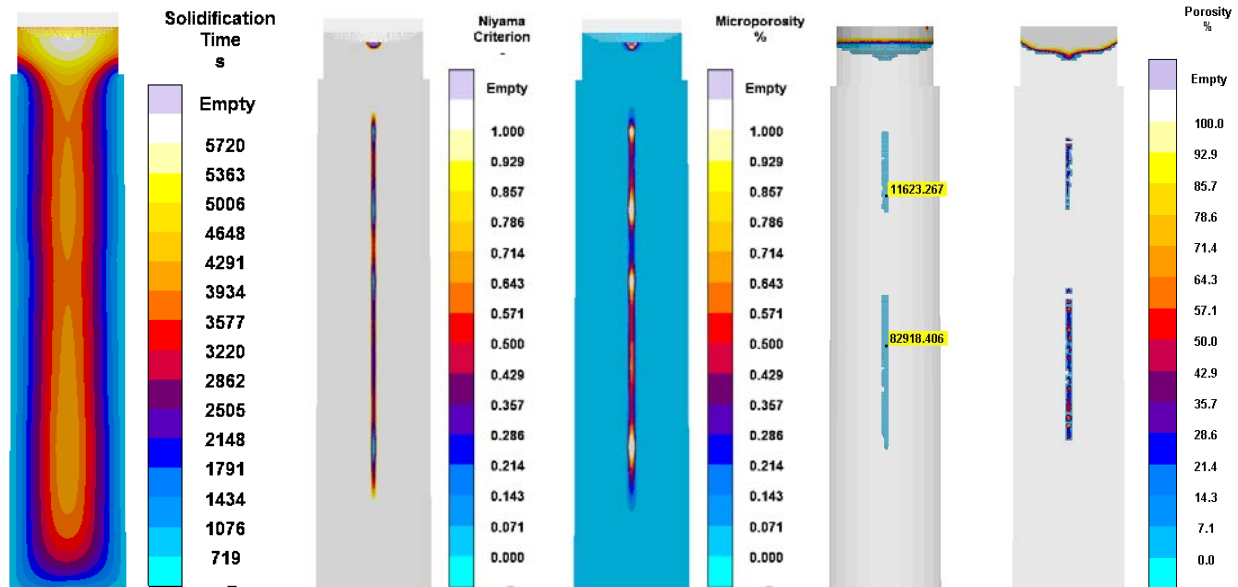


Fig. 8(a) Local solidification time of the slim ingot. Two isolated liquid pools are seen, indicating issues with shrinkage porosity.

Fig. 8(b) Prediction of the centerline macro/micro shrinkage using the Niyama criterion. The information about the defect is qualitative.

Fig. 8(c) Prediction of the centerline macro/micro shrinkage based on the modified Niyama criterion. It quantifies the defect in %.

Fig. 8(d) Prediction of macroscopic shrinkage porosity due to improper solidification pattern and lack of feed metal.

4.2 Optimization results

The primary reason for autonomous optimization has been to find a more suitable design of the ingot, the hot top and optimal process conditions (filling temperature, flow rate profile) to minimize the presence and extent of solidification related issues such as centerline porosity and shrinkage porosity as seen in the original ingot layout.

Fig. 9 shows the results of the numerical optimization with all calculated designs for the considered ingot. Design (1) indicates the best design selected by the optimization and design (2) indicates the original ingot design. Since the reduction of the volume of shrinkage porosity was given the highest priority, the “best” design for this objective is therefore located at the right bottom corner. As compared to the original design (2) the optimized design (1) shows significant improvement in reducing the macro porosity, but the centerline shrinkage will get worse a bit. But in this study, the centerline porosity was not a major issue. In all segments, the shrinkage porosity, specifically its volume got reduced by the optimization but the situation with the centerline microporosity remained more or less the same. This confirms an assumption that it is almost impossible to reduce centerline shrinkage (on a micro scale) for slim and tall ingots. The design variables would have to be defined with much wider limiting values to achieve major improvement in this particular defect. This will be shown later in the text. Although it may seem from the Y-axis of **Fig. 9** that the value for the volume of macro porosity is zero, it is not. There is still some minor volume of shrinkage porosity present in the ingot, which is not clearly seen from the figure.

The selected design (1) is captured in **Fig. 10**. It is obvious that the ingot geometry together with the hot top got considerably modified. The optimized ingot expands upwards (V shape ingot), while the original ingot expanded downwards (A shape ingot). Also the hot top does not have a constant diameter but its bottom diameter is larger than the top diameter. The bottom diameter of the hot top is also larger than it used to be in the original design. All this should lead to significant improvement in the internal soundness of the given ingot. The exact comparison with the original solution in terms of design variables can be seen in **Fig. 11** and in **Table IV**.

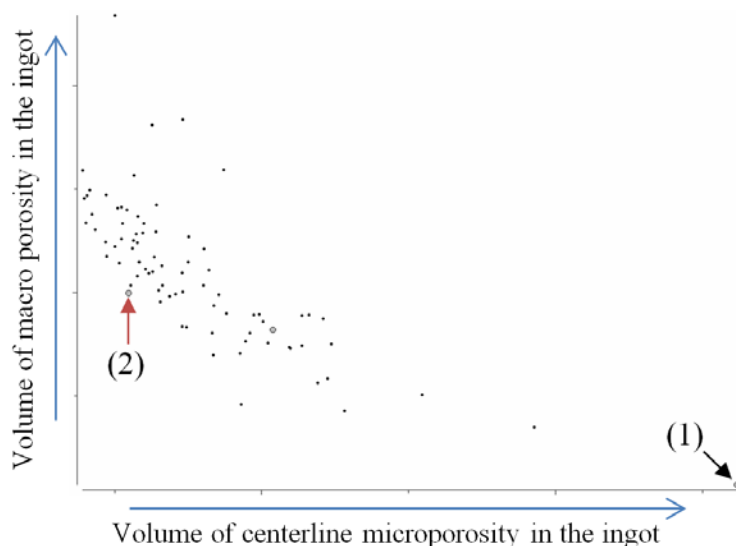


Fig. 9 Volume of porosity versus volume of centerline porosity for the considered ingot: black dots show the calculated designs. Design (1) indicates the best design selected by the optimization and design (2) indicates the original ingot design. The blue arrows imply in which direction the values on the axes are growing. The zero value is at the origin of the axes.

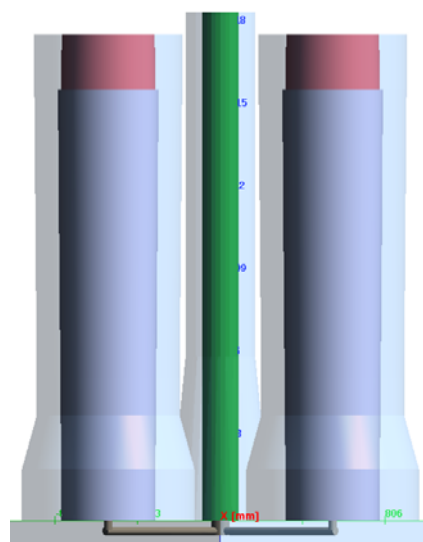


Fig. 10 New ingot casting layout after optimization. Dimensions of the hot top, the actual ingot body and process parameters were varied during optimization.

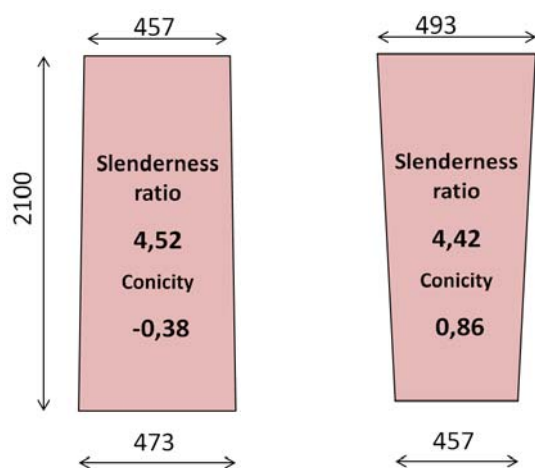


Fig. 11 Comparison of the original (left) and the optimized (right) ingot geometry.

Table IV Optimized values of the design variables

Design variable	Original ingot	Optimized ingot
Filling temperature	1560 °C	1550 °C
Flow rate	2190 cm ³ /s	1930 cm ³ /s
D_ingot_bottom	473 mm	457 mm
D_ingot_top	457 mm	493 mm
D_hot top_bottom	410 mm	463 mm
D_hot top_top	410 mm	453 mm
Height_hot top	250 mm	270 mm

The new solidification behavior is captured in **Fig. 12**. The optimized ingot geometry induced more directional solidification towards the hot top. Because of the positive conicity (the so-called V-shape ingot), the bottom section of the ingot no longer solidifies later than the middle section as it was the case at the original ingot, see **Fig. 7**. Even at the later stages of the solidification interval, no separation or choking of residual liquid can be seen. This is also confirmed on **Fig. 13** showing the local solidification time. The new solidification pattern should minimize the risk of macroscopic shrinkage defects.

As already seen in **Fig. 13**, the large areas with the same solidification time imply that those areas will solidify at the same time and in the same manner. This means that there will be no distinct direction for the heat removal, thus, a flat thermal gradient. As a consequence, large and coarse equiaxed solid grains (dendrites) will be present in the centerline of an ingot. The optimized geometry together with the optimized process conditions will lead finer microstructure at the centerline as compared to the original ingot casting which will minimize the permeability of the mush and the subsequent micro pores will be smaller and widely distributed along the centerline. This phenomenon can be seen if one compares **Figs. 8(b, c)** with **Figs. 14(a, b)**. The optimized ingot should yield higher internal soundness than the original. Note that for this type of ingots, i.e. slim and tall, it is virtually impossible to completely avoid centerline microporosity. The geometry would have to look completely different, i.e. with much higher positive conicity to induce steeper thermal gradients which would eliminate the given defect. In fact, the optimization clearly confirmed this statement. The optimal design of the ingot can be macroporosity free as seen in **Fig. 14(c)**, but the centerline microporosity will always be there, but its distribution will be more favorable.

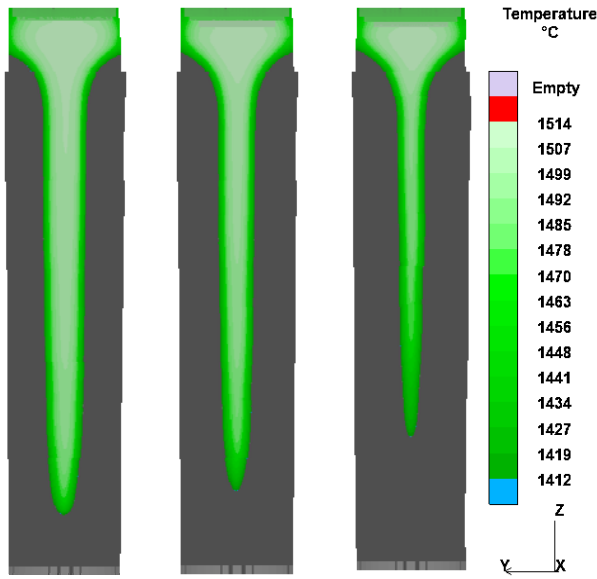


Fig. 12 Solidification behavior of the optimized ingot at three time steps showing more progressive and directional pattern as compared to the original A-shape ingot. No signs of choking off liquid pools are seen.

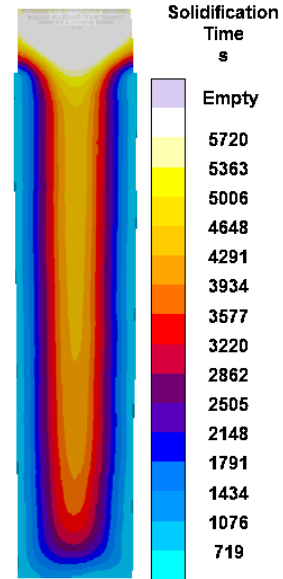


Fig. 13 Prediction of local solidification time for the optimized ingot. Although the shrinkage porosity due to lack of feeding will be reduced, the problems with flat thermal gradients will persist in the centerline giving rise to coarse equiaxed grain structure with isolated microporosity.

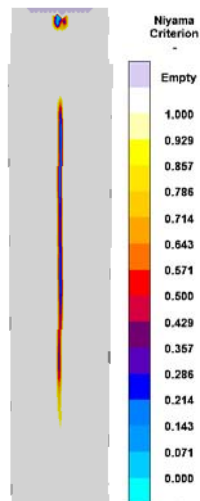


Fig. 14(a) Prediction of the centerline macro/micro shrinkage using the Niyama criterion for the optimized ingot geometry

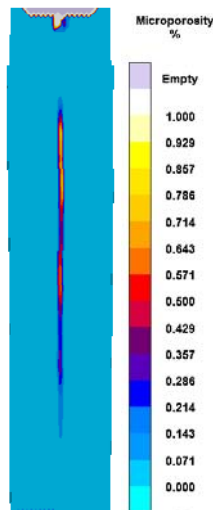


Fig. 14(b) Prediction of the centerline macro/micro shrinkage based on the modified Niyama criterion for the optimized ingot geometry.

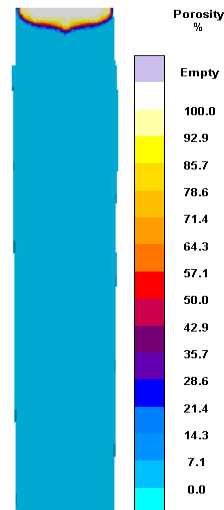


Fig. 14(c) Prediction of macroscopic shrinkage porosity. The ingot body seems porosity free. The major shrinkage is located in the hot top as an open shrink.

Last step of the optimization procedure was an analysis of how much the given design variables influence the optimization objective, i.e. how sensitive the given objective is towards the variation of the individual design variables. It follows that the most decisive design variables are the bottom and the top diameters of the ingot body together with the diameters of the hot top. In other words, the type of the ingot conicity together with the shape of the hot top have much bigger impact on the reduction of the macro porosity than the flow rate profile and the teeming temperature. This valuable finding will serve as a reference for future optimization studies. If one could use only the geometrical design variables and could leave out the process parameters, i.e. the flow rate profile and the teeming temperature, from the optimization, it would simplify the optimization procedure and lead to shorter calculation times.

The results of the optimization study have been presented to the management of the involved foundry for their consideration. As a next step it has been decided by the foundry to apply the optimization findings in the real casting experiments to correlate the numerical predictions with reality.

5. Conclusions

The aim of this study has been to find a more suitable design of the ingot body, its hot top and optimal process conditions (filling temperature and flow rate profile) using the autonomous optimization tool, to minimize the presence and extent of solidification related issues such as shrinkage porosity and centerline microporosity as seen in the original ingot layout. The objective space for the considered optimization problem has been constructed by the predefined objective: Minimization of the volume of shrinkage porosity and three other constraints which have been addressed earlier in the text.

Results of the optimization procedure have shown that the shape of the ingot, mainly its conicity (A-shape vs. V-shape) and the slenderness ratio are by far the most decisive factors in reducing the feeding related issues such as macroporosity. Together with the optimized shape of the hot top and process conditions it was possible to completely minimize the macroporosity. However, another very common defect in ingot castings, the centerline microporosity predicted by the well-known Niyama criterion has shown to be resistant to the given optimization measures. This is because of the constraints in the design variables which would have to be more open to cause significant improvement in this defect. The thermal gradient which stands behind the formation of centerline shrinkage cannot be significantly increased by the applied optimization changes. Nevertheless, there has been some minor improvement in minimizing the centerline shrinkage. It seems to be distributed more evenly over a larger area as compared to the original ingot. It means that the defect will be less problematic due to the more spread out pattern.

Acknowledgement

The work is supported by the Strategic Research Centre "REWIND - Knowledge based engineering for improved reliability of critical wind turbine components", Danish Research Council for Strategic Research, grant no. 10-093966, and by the research projects MPO FR-TI3/373 and FR-TI3/374

References

- [1] KOTAS, P., TUTUM, C.C., SNAJDROVA, O., THORBORG, J., HATTEL, J.H., „A Casting Yield Optimization Case Study: Forging Ram”, Int. Journal of MetalCasting, Vol. 4, Issue 4, (2010).
- [2] KOTAS, P., TUTUM, C.C., THORBORG, J., HATTEL, J.H., “Elimination of Hot Tears in Steel Castings by Means of Solidification Pattern Optimization”, Metallurgical and Materials Transactions B, Vol. 43, Issue 3, pp. 609-626, (2012).
- [3] KOTAS, P., HATTEL, J.H., “Modeling and simulation of A segregates in steel castings using thermal criterion function Part II – Optimisation of real industrial cast part”, Materials Science and Technology, Vol. 28, No. 8, (2012).
- [4] KOR, J., CHEN, X., HU, H., “Multi-Objective Optimal Gating and Riser Design for Metal-Casting”, 2009 IEEE International Symposium on Intelligent Control, Part of 2009 IEEE Multi-conference on Systems and Control, Saint Petersburg, Russia, July 8-10, (2009).
- [5] HAHN, I., HARTMANN, G., “Automatic computerized optimization in the die casting processes”, Casting Plant & Technology, Vol. 24, no. 4, (2008).
- [6] FLENDER, E. and STURM, J., “Thirty Years of Casting Process Simulation,” International Journal of Metalcasting, Spring 10, pp. 7-23, (2010).
- [7] KOTAS, P., PH.D. THESIS, Technical University of Denmark, Kgs. Lyngby, Denmark, (2011).
- [8] MAGMAfrontier 4.4 Reference Manual, (2005).
- [9] HAHN, I., HEPP, E., „Improved ingot casting by numerical simulation“, proc. ICRF 2012, Aachen, (2012).
- [10] GOLDBERG, D.E., “Genetic Algorithms in Search, Optimization & Machine Learning”, Addison Wesley Longman, Inc., (1989).
- [11] CARLSON, K.D., BECKERMANN, C. “Prediction of Shrinkage Pore Volume Fraction Using a Dimensionless Niyama Criterion”, Metallurgical and Materials Transactions A, Vol. 40A, pp. 163-175, (2009).